Generating Microlensing Magnification Maps

T. Petrović[1], **P. Jovanović**[2], **L. Č. Popović**[2]

[1]Department of Astronomy, Faculty of Mathematics, University of Belgrade,
 Studentski trg 16, 11000 Belgrade, Serbia

[2]Astronomical Observatory, Volgina 7, 11160 Belgrade 74, Serbia

Abstract. We present here the ray-shooting method for generating microlens
magnification maps. We generated several examples and discussed influence
of the parameters of quadruple microlenses on generated maps. Particulary we
generated the maps for gravitational lens systems PG1115+080 and B1422+231.

1 Introduction

Optical, UV and X-ray spectra observations of the lensed quasars show flux ratio
anomalies among the images (see Maccio & Miranda 2006 [1], Blackburne *et
al.* 2006 [2], Dobler & Keeton 2006 [3] and references therein). It has proven
difficult in many cases to match the flux ratios among the images predicted by
lens models, to those actually observed. Small-scale structure is often invoked to
explain these flux ratio anomalies, either in the form of microlensing by stars or
millilensing by dark matter subhaloes. Another potential source of flux anoma-
lies is differential extinction in the lensing galaxy.

Our aim in this paper is to investigate these flux anomalies by modeling Op-
tical, UV and X-ray continuum as emitted from an accreation disc (Popović
et al. 2006 [4]) amplified due to microlensing in the particular lens systems
B1422+231 and PG1115+080.

2 Generating Microlensing Magnification Maps

For generating microlens magnification maps we used the ray-shooting method
(Schneider *et al.* 1986, 1987, [5] & [6]). The input parameters are average sur-
face mass density κ, shear γ and width of microlensing magnification map ex-
pressed in units of Einstein radius (defined for one solar mass in the lens plane).

Firstly, we generate random star field in the lens plane with use of parameter κ.
Next is solving the Poisson equation $\nabla^2 \psi = 2\kappa$ in the lens plane numericaly,
so we can determine the lens potential ψ in every point of the grid in the lens
plane. To solve the Poisson equation we must write the finite difference form

of the equation and invert the equation using Fourier techniques. After some derivation we obtain:

$$\hat{\psi} = \frac{\hat{\kappa}_{mn}}{2(\cos \dfrac{m\pi}{N_1} + \cos \dfrac{n\pi}{N_2} - 2)}, \tag{1}$$

where N_1 and N_2 are dimensions of the grid in the lens plane. So, solving the Poisson equation consists of three steps:

1) find the Fourier component $\hat{\kappa}$ by taking discrete Fourier transformation of κ

2) calculate Fourier component $\hat{\psi}$ using the equation (1)

3) compute ψ by taking an inverse Fourier transform of $\hat{\psi}$

Now, using the finite difference technique, we can compute the deflection angle $\vec{\alpha} = \nabla \psi$ in each point of the grid in the lens plane.

After computing deflection angle, we can the regular grid of points in the lens plane, via lens equation, map onto the source plane. These light rays are then collected in pixels in the source plane, and the number of rays in one pixel is proportional to the magnification due to microlensing at this point in the source plane. Advantage of use Fourier techniques is it's number of operations $N \lg N$ which is much less than number of operations in conventional methods N^2 (N is dimension of the grid in the lens plane).

3 Results

We estimate average surface mass density κ and shear γ of all quasar's images with use of the singular isotheral ellipsoid (SIE) gravitational lens models B1422+231 in Korman *et al.* (1994) [7] and PG1115+080 in Chiba (2002) [8]. The results are given in Table 1.

Table 1. Average surface mass density κ and shear γ at the positions of the quasar's images in the lens systems B1422+231 and PG1115+080.

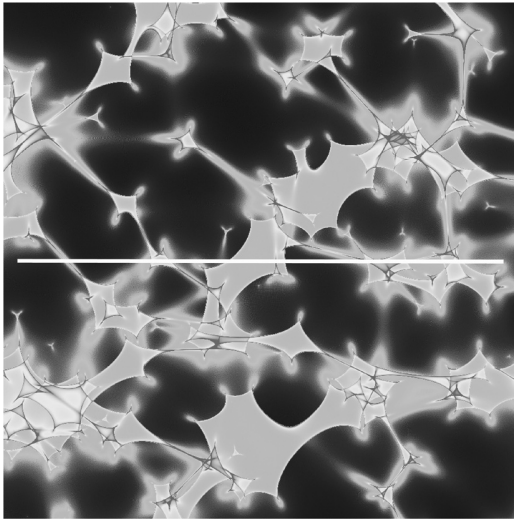| B1422+231			B1115+080		
image	κ	γ	image	κ	γ
A	0.42	0.1	A_1	0.56	0.11
B	0.38	0.1	A_2	0.63	0.11
C	0.37	0.1	C	0.85	0.11
D	3.32	0.1	D	0.45	0.11

Figure 1. Microlensing magnification map in the source plane, produced by a dense field of stars in the lensing galaxy of B1422+231 image B ($\kappa = 0.38$, $\gamma = 0.1$). The width of the map is 16 Einstein radii or 42200 gravitational radii. The grey tone reflects the magnification as a function of the quasar position: the sequence black-grey-white indicates increasing magnification. Amplification variations taken along the solid white line are shown in Figure 2.
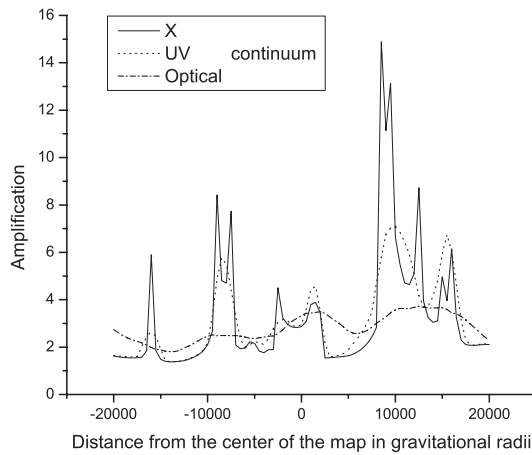

Figure 2. Amplification variations for different positions of the accretion disk center along the solid white line in Figure 1. The solid, dotted and dash-dotted line indicate amplification variations for X-ray, UV and optical continuum, respectively.
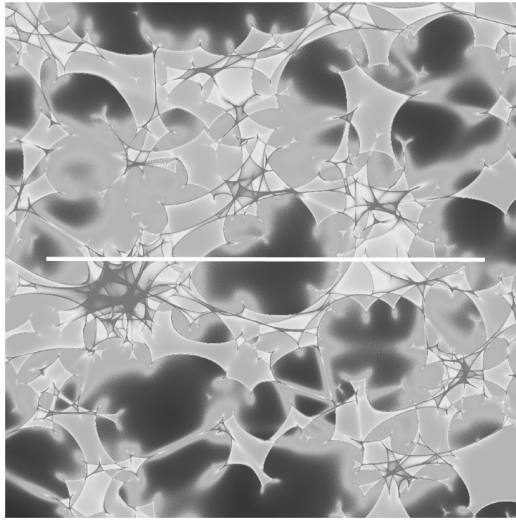
Figure 3. Microlensing magnification map in the source plane, produced by a dense field of stars in the lensing galaxy of PG1115+080 image C ($\kappa = 0.45$, $\gamma = 0.11$). The width of the map is 16 Einstein radii or 59600 gravitational radii. The grey tone reflects the magnification as a function of the quasar position: the sequence black-grey-white indicates increasing magnification. Amplification variations taken along the solid white line are shown in Figure 4.
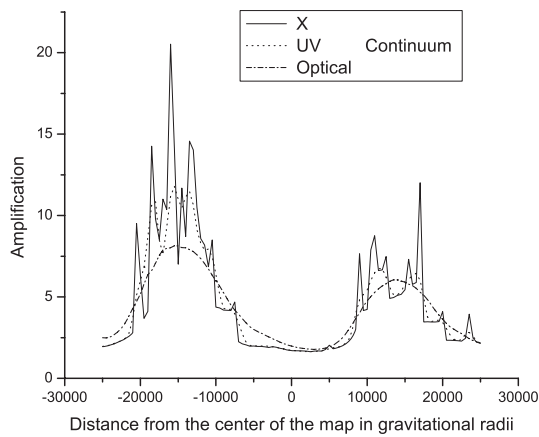

Figure 4. Amplification variations for different positions of the accretion disk center along the solid white line in Figure 3. The solid, dotted and dash-dotted line indicate amplification variations for X-ray, UV and optical continuum, respectively.

The disc emission was analyzed using numerical simulations based on a ray-tracing method in a Kerr metric, taking into account only photon trajectories reaching the observer's sky plane.

Here we present in Figures 1 and 3 microlens magnification maps of B1422+231 image B and PG1115+080 image C, respectively and corresponding amplification variations along the solid white line in X-ray, UV and optical continuum are presented in Figures 2 and 4.

As one can see from the Figures 2 and 4, the X-ray continuum amplification due to microlensing is significantly larger than one in the optical and UV continua. Also, due to compact size of X-ray continuum emitting region, its variations are the fastest.

References

[1] A.V. Maccio, M. Miranda (2006) *MNRAS* **386** 599.

[2] J.A. Blackburne, D. Pooley, S. Rappaport (2006) *ApJ* **640** 569.

[3] G. Dobler, C.R. Keeton (2006) *MNRAS* **365** 1243.

[4] L.Č. Popović, P. Jovanović, E. Mediavilla, A.F. Zakharov, C. Abajas, J.A. Munoz, G. Chartas (2006) *ApJ* 637 620–630.

[5] P. Schneider, A. Weiss (1986) *Astr. Ap.* **164** 237.

[6] P. Schneider, A. Weiss (1987) *Astr. Ap.* **171** 49–65.

[7] R. Kormann, P. Schneider, M. Bartelmann, (1994) *A&A* **286** 357.

[8] Chiba, Masashi, (2002) *ApJ* **565** 17.